



International Commission on Illumination
Commission Internationale de l'Eclairage
Internationale Beleuchtungskommission

A MATHEMATICAL FRAMEWORK FOR COMPARING PHOTOMETRIC OBSERVERS

Bergen, A.S.J., and Schneider, T.

DOI 10.25039/x051.2025/4nq5uj

This article is also published as part of:

Proceedings of the CIE 2025 Midterm Meeting Vienna, Austria, July 4-11, 2025:
Scientific Conference (July 7-9, 2025)

DOI 10.25039/x051.2025

in

Proceedings of the CIE (International Commission on Illumination)

ISSN no. 3061-015X (print), 3061-0168 (online)

The paper has undergone double-blind peer review and its final version has been presented at the CIE 2025 Midterm Meeting, Vienna, Austria, July 4–11, 2025.

© CIE 2025

All rights reserved. This work is licensed under the Creative Commons Attribution-NonCommercial 4.0 International License (<https://creativecommons.org/licenses/by-nc/4.0/>). Any mention of organizations or products does not imply endorsement by the CIE.

CIE Central Bureau
Babenbergerstrasse 9/9A
A-1010 Vienna, Austria
Tel.: +43 1 714 31 87
e-mail: ciecb@cie.co.at — www.cie.co.at

A MATHEMATICAL FRAMEWORK FOR COMPARING PHOTOMETRIC OBSERVERS

Bergen, A.S.J.^{1,3}, Schneider, T.²

¹ Photometric Solutions International, Melbourne, AUSTRALIA, ² Instrument Systems GmbH, Munich, GERMANY, ³ Australian Photometry and Radiometry Laboratory, Melbourne, AUSTRALIA

t.schneider@instrumentsystems.com

Abstract

The $V(\lambda)$ function, a photometric observer representing the spectral luminous efficiency of human vision, has been the basis of photometry for 100 years. Cone fundamentals offer an alternative to $V(\lambda)$, $V_F(\lambda)$, which is accepted as a better match to human vision. In addition, the framework of cone fundamentals allows parametrization of $V_F(\lambda)$ to account for the significant diversity among human populations, e.g. for changes as we age and also changes with respect to field-of-view. There is currently a debate about the potential benefits of changing the normative photometric observer, defining the photometric units, from $V(\lambda)$ to a cone fundamental based observer, e.g. $V_F(\lambda)$.

A change from $V(\lambda)$ to any other reference observer would require good justification as it would have profound consequences for measurement technology, metrology and the photometric unit scale. This paper introduces a mathematical framework for comparing one observer against another observer, across observer populations and lighting applications.

Keywords: Photometry, Cone fundamentals, Photometric observers

1 Introduction

The $V(\lambda)$ function, a photometric observer representing the spectral luminous efficiency of human vision in photopic conditions, has been the basis of photometry for 100 years since its adoption by the CIE in 1924 (CIE, 1926). It is well known that $V(\lambda)$ is not perfect, and in particular it underestimates the response significantly in the shorter wavelengths. Still, it has served well as the basis for photometric units and to establish comparability of measurement results. Over time CIE introduced additional observers better matched to particular viewing conditions, e.g. for scotopic vision or for a field of view of 10° . So, while is by no means the only observer available, it still defines the photometric units, e.g. any reading of lumen or candela is expected to be related to spectral weighting by $V(\lambda)$, if not explicitly stated otherwise.

In 2006, the CIE published a system of cone fundamentals (CIE, 2006), in which the spectral luminous efficiency function of human vision can be calculated for ages ranging from 20 years to 80 years old, and for fields of view ranging from 1° to 10° . Thus, a specific spectral responsivity function can be calculated for a typical person of a specific age and for a specific application, thereby allowing the capture of important aspects of the observed diversity in human vision.

In 2015, the CIE published an extension to this system of cone fundamentals, and proposed a particular cone-fundamental-based spectral luminous efficiency function for a 32 year old observer using a 2° field size in terms of energy (CIE, 2015). This alternative function, $V_F(\lambda)$, has a higher response in the short wavelength region and is therefore considered to be a better physiological match than $V(\lambda)$ for photopic vision.

A change in the basis of photometry from $V(\lambda)$ to $V_F(\lambda)$ could potentially have dramatic effects. For broadband photometers, which have fixed physical structures in the form of $V(\lambda)$ filters that adapt their spectral responsivity to match the required function, a change to $V_F(\lambda)$ would mean that the instrument would either need to be discarded and replaced, or that some correction

would need to be made to measured data to adapt the reading to the correct function. A change to $V_F(\lambda)$ would also result in a change in the scale of luminous quantities of the order of 5 % for most white light sources, or alternatively a change in the defining constant used for photometry, K_{cd} (Shitomi, 2023).

Any of these changes will result in significant costs in terms of the replacement of instruments and the administrative time taken to make changes to standards, regulations and processes. It would likely take close to a generation to transition and is likely be accompanied by significant confusion. Therefore, a potential change of the normative photometric observer requires careful consideration, weighing the potential benefits with respect to an improved physiological match against the unavoidable problems for metrology.

In view of the diversity of physiological photometric observers, important questions arise. How does the spectral spread in observers compare to the spectral differences between $V(\lambda)$ and $V_F(\lambda)$? How does the spectral spread impact human perception in different applications? What would be an optimal “average” observer across human population and applications to replace $V(\lambda)$ in the definition of photometric units and what should “optimal” mean in this context?

Addressing those questions requires a mathematical framework that allows comparison of observers in different applications. This paper introduces a set of metrics: Two photometric observer mismatch indices (OMI) and the photometric observer mismatch factor (OMF). These provide a mathematical framework for evaluating one observer against another observer, i.e. $V_F(\lambda)$ with respect to $V(\lambda)$, with respect to a single spectral distribution. This is then extended to evaluate the two observers across multiple spectral distributions, across whole populations, and across multiple applications.

2 Variation in cone fundamental based photometric observers

The CIE system of cone fundamentals currently includes parametrization of spectral luminous efficiency functions (“photometric observers”) with respect to the field of view and a person’s age and in principle allows addition of additional parameters in the future. While the parametrization is a requirement for an improved physiological description of (ultimately) individual human brightness perception under particular lighting conditions.

As a necessary consequence there is no longer a single unique reference photometric observer in the cone fundamental system. A proposed reference photometric observer potentially to replace $V(\lambda)$ in the future corresponds to the cone fundamental observer closest to $V(\lambda)$, that is the one for a 2° field of view and an age of 32 years. Independent of the question “what would be the “best” reference observer to define photometric units”, the intrinsic spectral variability of photometric observers in CIE system of cone fundamentals requires a mathematical framework for quantitative comparison of different observers.

Figure 1 shows the typical spectral variation expected in cone-fundamental-based photometric observers V_{cf} as a function of age for a 2° field of view. The right graph clearly shows the well-known major “deficiency” of $V(\lambda)$ of strongly underestimating the photopic responsivity at short wavelengths, which is the main practical reason behind the discussion about a replacement of $V(\lambda)$ as the standard photometric observer to be used in the definition of photometric units. It can also be seen from the right graph that the variation of observer spectral differences with age is much larger than the spectral difference between $V(\lambda)$ and $V_F(\lambda)$ (magenta curve), illustrating the fact that in the cone fundamental system there is no obvious single reference observer and $V_F(\lambda)$ does not represent the centre of the age distribution of the 2° cone fundamental observers.

Note: In some places throughout this paper, $V(\lambda)$ is notated as $V_\lambda(\lambda)$ or V_λ .

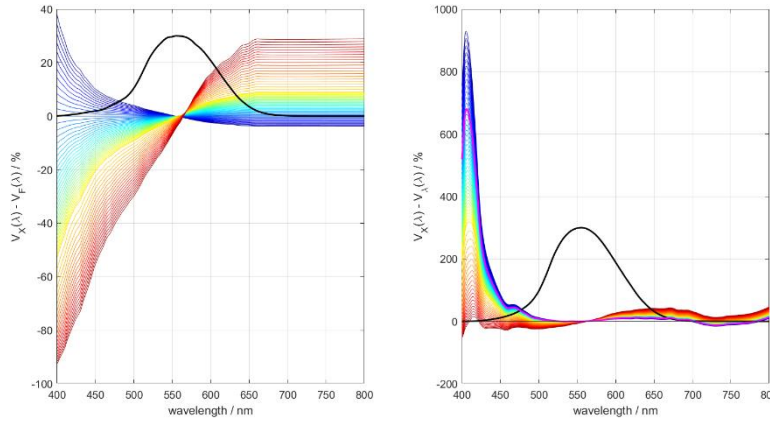


Figure 1 - Relative spectral differences of possible cone fundamental based photometric observers to reference observers $V_F(\lambda)$ (left graph) and $V_\lambda(\lambda)$ (right graph). Age increases from blue to red and ranges from 20 years to 80 years. Black curves illustrate the spectral distributions of V_F (left graph) and V_λ (right graph), respectively.

3 Photometric observer comparison metrics

The differences between two hypothetical photometric observer functions (or any other two spectral distributions) $V_1(\lambda)$ and $V_2(\lambda)$ are fully characterized by the spectral differences $\Delta V_{abs}(\lambda) = V_2(\lambda) - V_1(\lambda)$. For an easy practical comparison of observers, it is often advantageous to use scalar measure(s) of “closeness”, typically defined as weighted integrals over the spectral difference $\Delta V_{abs}(\lambda)$ or their absolute values. The appropriate meaning of “closeness” will be application dependent, e.g. in some context the maximum spectral difference might be important, while in another the mean spectral difference could be of interest. Therefore, there is no unique scalar measure for the comparison of spectral distributions that will be “optimal” for all applications. Here we propose three scalar measures for the comparison of photometric observers.

3.1 Photometric observer mismatch factor F_V

We define the observer mismatch factor (OMF) as the relative difference of photometric values for two photometric observers:

$$F_V(V_{ref}, V_X, S) = \frac{V_{ref}(\lambda_{cd})}{V_X(\lambda_{cd})} \cdot \frac{\int_{360nm}^{830nm} S(\lambda) \cdot V_X(\lambda) d\lambda}{\int_{360nm}^{830nm} S(\lambda) \cdot V_{ref}(\lambda) d\lambda} \tag{1}$$

where

- F_V is the photometric observer mismatch factor;
- $S(\lambda)$ is the spectral distribution used for the evaluation;
- $V_{ref}(\lambda)$ is the spectral distribution for a reference observer, normalized to its maximum value;
- $V_X(\lambda)$ is the spectral distribution for a comparison observer, normalized to its maximum value;
- λ_{cd} is the wavelength in standard air corresponding to a frequency of $540 \cdot 10^{12}$ Hz given in the definition of the SI-unit candela. $\lambda_{cd} \cong 555,017 \text{ nm}$

Note: Where the complete wavelength range is not available for all parameters, an abbreviated wavelength range should be used which corresponds to the shortest wavelength range present.

F_V directly measures the relative difference in the photometric integral (perceived brightness) for two photometric observers for a given spectral distribution $S(\lambda)$. The OMF is zero for $V_X(\lambda) = V_{ref}(\lambda)$. Examples of F_V for observers $V_F(\lambda)$ and $V_\lambda(\lambda)$ for example spectra are shown in Figure 2. Since spectral differences of different sign in different spectral regions can compensate each other in the calculation of F_V , spectrally very different observers can still lead to small values of F_V . The OMF therefore does not quantify the spectral differences of the two observers, but measures the effect of the observer spectral difference in a photometric measurement of a spectral distribution. The OMF explicitly includes a change in the maximum luminous efficacy

value. The analysis in (Shitomi 2023) uses a metric equivalent to F_V . Figure 2 shows how the OMF F_V changes with age for a fixed 2° field of view and 3 mm pupil diameter for $V_F(\lambda)$ and $V(\lambda)$, for five LED spectra taken from CIE 015:2018 (CIE, 2018).

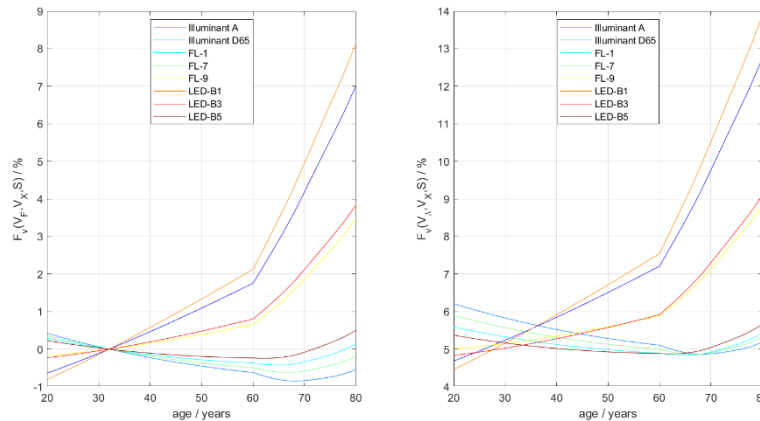


Figure 2 - Photometric observer mismatch factor F_V as a function of age for example standard CIE spectral distributions, evaluated for $V_F(\lambda)$ (left) and for $V(\lambda)$ (right).

3.2 Photometric observer mismatch index f_V

Ferrero et al (FERRERO, 2019) introduced the concept of a spectral mismatch index which was adopted into CIE 251:2023 as a spectral distribution mismatch index (CIE, 2023). A modified version of this is proposed here as a photometric observer mismatch index (OMI):

$$f_V(V_{ref}, V_X, S) = \int_{360\text{ nm}}^{830\text{ nm}} \left| \frac{S(\lambda)V_{ref}(\lambda)}{\int_{360\text{ nm}}^{830\text{ nm}} S(\lambda)V_{ref}(\lambda)d\lambda} - \frac{S(\lambda)V_X(\lambda)}{\int_{360\text{ nm}}^{830\text{ nm}} S(\lambda)V_X(\lambda)d\lambda} \right| d\lambda \quad (2)$$

where

- f_V is the photometric observer mismatch index for a given comparison observer;
- $S(\lambda)$ is the spectral distribution used for the evaluation;
- $V_{ref}(\lambda)$ is a reference observer;
- $V_X(\lambda)$ is a comparison observer

The OMI f_V , which is symmetric with respect to V_{ref} and V_X , compares the relative spectral distributions of the observer functions, normalized to their respective “photometric integrals”, weighted by a particular spectral distribution $S(\lambda)$. The normalization of the observer functions is chosen such, that for the case that either one of the observer functions is strictly zero, $f_V \rightarrow 1$, corresponding to a mean spectral difference of one hundred percent.

For the limiting case of $S(\lambda) = \text{constant}$, f_V compares the relative observer functions (normalized to their respective integrals) directly. The introduction of the additional weighting by the spectral distribution $S(\lambda)$ allows evaluation of the relevance of the spectral differences in the observer functions with respect to a particular application of interest, represented by $S(\lambda)$.

In general, f_V will increase with increasing spectral bandwidth of the source spectrum considered, as then spectral differences between observers from a larger spectral range will contribute to the value of f_V .

The normalization of the observers to their respective “photometric integrals” (up to maximum luminous efficacy constants) makes f_V a “complementary” metric to F_V in the sense, that f_V is expected to be typically weakly correlated with F_V , except for smooth spectral distributions like, for example, for incandescent lamps.

As a consequence of the normalization in (2), the mismatch index is small whenever the spectral difference (over the range of significant spectral amplitude of $S(\lambda)$) between the two observer

functions is mostly due to a common scaling factor. In this case, the two observers would represent essentially the same relative spectral weighting for a given $S(\lambda)$ and therefore could be regarded as equivalent. The mismatch index is strictly zero for monochromatic light ($S(\lambda) = \delta(S(\lambda - \lambda_0))$). The mismatch index (2) is therefore well suited to compare photometric observers with respect to an individual spectrum $S(\lambda)$, but not to compare them with respect to a set of spectra. As an example, consider an application based on a set of essentially monochromatic spectra, e.g. a trichromatic laser display. Since the individual spectra are monochromatic, the mismatch indices will be very small for each of them as at single individual wavelengths the observer functions are always related by a scaling factor that is, in general, specific for that wavelength. For a superposition of any of the spectra (e.g. the aforementioned display set to “white”) on the other hand, the mismatch index can be quite large as there will in general be no longer a common scaling factor relating the two observer functions at multiple wavelengths. The value of the mismatch index will in this case be related to the differences in the scaling factors at the individual wavelengths.

Figure 3 shows how the OMI f_V changes with age for a fixed 2° field of view and 3 mm pupil diameter for $V_F(\lambda)$ and $V(\lambda)$, for five LED spectra taken from CIE 015:2018 (CIE, 2018). The numbers are a little contrived, since $V_F(\lambda)$ is defined for an age of 32 years and 2° field of view, hence the mismatch index here is zero, however the trend that the mismatch increases with age is clear. It is also possible to apply the same principle but keep the age of the observer the same and change the field of view.

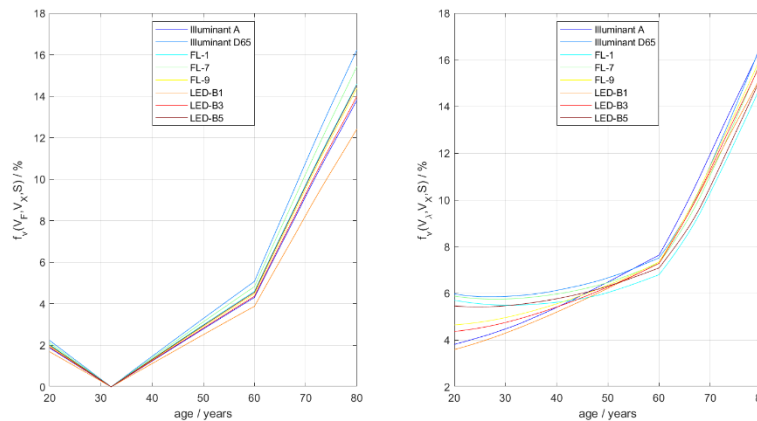


Figure 3 - Photometric observer mismatch factor f_V as a function of age for example standard CIE spectral distributions, evaluated for $V_F(\lambda)$ (left) and for $V(\lambda)$ (right)

3.3 Photometric observer mismatch index f_{V2}

We also propose a slightly different OMI based on the absolute spectral differences weighted by the relative spectral distribution of a light source of interest, given by

$$f_{V2}(V_{ref}, V_X, S) = \int_{360\text{ nm}}^{830\text{ nm}} \frac{S(\lambda)}{\int_{360\text{ nm}}^{830\text{ nm}} S(\lambda') d\lambda'} |V_X(\lambda) - V_{ref}(\lambda)| d\lambda \tag{3}$$

where

- f_{V2} is the photometric observer mismatch index for a given comparison observer;
- $S(\lambda)$ is the spectral distribution used for the evaluation;
- $V_{ref}(\lambda)$ is the spectral distribution for a reference observer, normalized to its maximum value;
- $V_X(\lambda)$ is the spectral distribution for a comparison observer, normalized to its maximum value;

The OMI f_{V2} is a weighted average of the absolute spectral differences between the spectral distributions of the two observers. In the limiting case $S(\lambda) = constant$, f_{V2} is simply the mean absolute spectral difference. The introduction of the additional weighting by the spectral

distribution $S(\lambda)$ allows evaluation of the relevance of the spectral differences in the observer functions with respect to a particular application of interest, represented by $S(\lambda)$. By standard convention, the spectral distributions for photometric observers are non-negative and required to be normalized to their respective maximum values. The spectral differences in (1), and thereby the values for f_{V2} , are then limited to the interval $[0,1]$.

For a set or superposition of several spectra ($S(\lambda) = \sum_i c_i \cdot S_i(\lambda)$) f_{V2} is, in contrast to f_V , also a linear average with respect to the spectral distributions, making it often more suitable to analyse sets of spectra. As it does not normalize the observers to a photometric integral, f_{V2} is expected to be in general be more correlated with F_V than f_V .

Examples of f_{V2} versus age for observers $V_F(\lambda)$ and $V_\lambda(\lambda)$ for example spectra are shown in Figure 4.

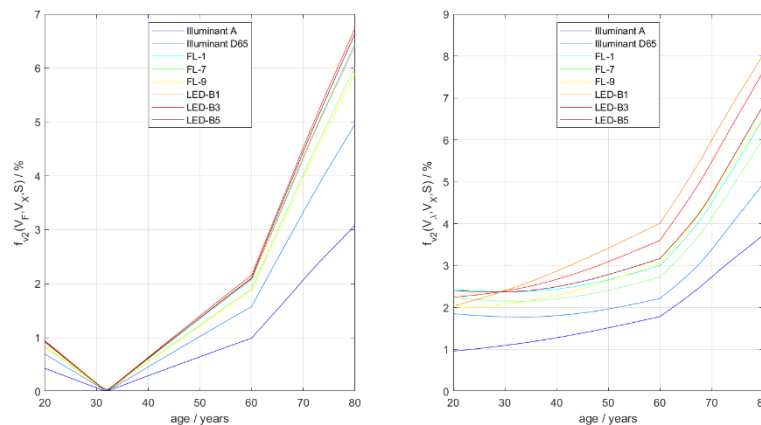


Figure 4 - Photometric observer mismatch factor f_{V2} as a function of age for example standard CIE spectral distributions, evaluated for $V_F(\lambda)$ (left) and for $V_\lambda(\lambda)$ (right)

3.4 Observer mismatch metric comparison

Figure 4 shows values for the observer mismatch metrics f_V , f_{V2} and F_V calculated for observers $V_F(\lambda)$ and $V_\lambda(\lambda)$ for example LED spectra.

The OMI f_V effectively evaluates relative differences up to a global scaling over the spectral range covered by the test spectrum S . As can be seen from the right graph of Figure 5, the relative spectral observer difference is significant, but almost constant across the spectrum of the example red LED, leading to a small value for f_V for the red LED, while the value for the blue LED is large as the relative observer difference is large and strongly varying over the spectrum of the blue LED. The value for the green LED is small as observer functions match well over its spectral range. For the white L41 spectrum, the relative spectral observer difference is strongly varying over the spectrum and therefore all differences contribute to the weighted average f_V , leading to a value close to the mean of the f_V -values for the blue-, red- and green LED.

f_{V2} is a weighted average of the absolute differences of the observer functions. Therefore, the values for the red- and blue LED are very similar (see left graph of Figure 5). As for f_V , the value is small for the green LED, for which the spectral differences are small over its spectral range, and the value for L41 is slightly above the mean of f_{V2} -values for the blue-, red- and green LED.

The observer mismatch correction factor F_V directly compares the photometric values that would be obtained for a given spectrum for the two observers. It is sensitive to the relative spectral differences, but spectral differences of different sign in different wavelength regions can compensate each other. Other than f_V , F_V accounts also for constant relative spectral differences. Therefore, it gives large values also for the red LED (other than f_V). In contrast to f_{V2} , the values for the blue and red LED differ, because the relative spectral differences in the blue spectral range are larger than in the red spectral range. In contrast to the other two metrics, F_V is a signed quantity.

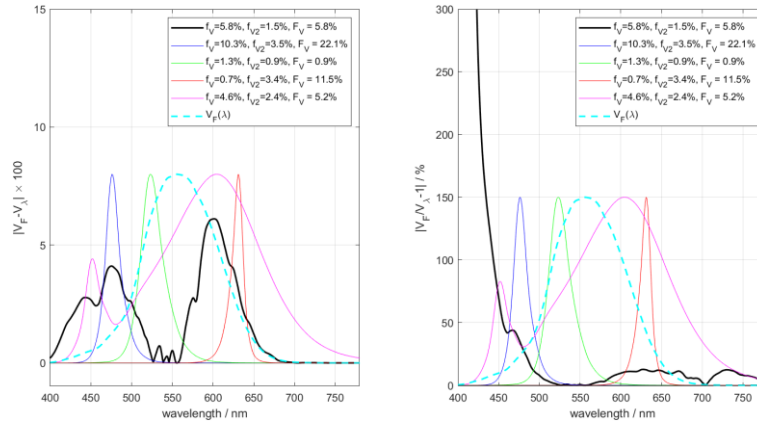


Figure 5 - Mismatch metrics values in percent for observers $V_F(\lambda)$ and $V_\lambda(\lambda)$ for example spectra. Black curve: Absolute (left graph) and relative (right graph) spectral observer difference, metrics are calculated using $S(\lambda)=1$. Red, yellow and purple curves: single colour LED spectra. Green curve: CIE L41. Cyan dashed line: photometric observer V_F . Spectra and V_F are shown in arbitrary units for illustration purposes only.

The observer mismatch indices f_V and f_{V2} also allow comparison of the spectral distributions of observers directly without reference to a particular test spectrum by setting $S(\lambda) = 1$. In this case, f_V and f_{V2} are essentially equivalent in the sense that the values for the two indices are strongly correlated independent of the observers considered.

As a consequence of the normalization of f_V in (2) f_V will typically be less correlated with F_V than f_{V2} . For smooth broadband distributions (e.g. halogen lamp spectra) all three metrics will typically be strongly correlated.

4 Statistical analysis for populations and applications

In order to evaluate observer differences for sets of spectra (e.g. characteristic for a particular application, like the primaries of a display) or populations (e.g. age class structures) we introduce the weighted average

$$\langle X_V \rangle_P = \frac{\sum_{p \in P} X_{V,p}(V_{ref}, V_{X,p}, S_p) \cdot w(p)}{\sum_p w(p)} \tag{4}$$

where

- $X_{V,p}$ is the value of a metric (e.g. f_V , f_{V2} or F_V) for a particular set of parameters $p \in P$ (e.g. age $V_{X,age}$ or/and a specific spectrum S_p);
- $w(p)$ relative weight associated with $X_{V,p}$;

We also introduce the following metric to characterize the spread in values for a metric across sets of spectra and/or populations

$$\Delta_P(X_{V,p}) = \max_{p \in P} (X_{V,p}(V_{ref}, V_{X,p}, S_p)) - \min_{p \in P} (X_{V,p}(V_{ref}, V_{X,p}, S_p)) \tag{5}$$

A “min-max” metric is chosen for the analysis of the effects of observer variation as the evaluation should allow accounting for large differences even if they only affect a small amount of the population. If “outliers” or parts of the population are to be excluded from an analysis, the analysis can be repeated for an appropriate subset of the population.

An interesting quantity for the analysis of observer differences across a population is the relative variation of a mismatch metric given by

$$\Delta_{p,rel}(X_V) = \frac{\Delta_P}{\langle X_V \rangle_P} \tag{6}$$

In this paper we focus on the investigation of the observer variance with age and its impact for example applications represented by sets of spectra. For a given spectrum, Δ_p will only depend on the range of ages considered, but not on the age class structure, while $\Delta_{p,rel}$ will vary with age class structure. $\Delta_{p,rel}$ can take on arbitrarily large values if $\langle X_V \rangle_p$ is close to zero. Figure 6 shows approximate distribution functions for idealized age class structures (“population pyramids”) typically used in demographics to characterize the age class structure of subsets of human population, e.g. of a country, labelled by commonly used “nicknames” (onion, bell, etc.) (see e.g. <https://de.wikipedia.org/wiki/Altersstruktur>, accessed 2025-04-30). For the following analysis, a potential difference in the age class structures of different sexes is ignored as the current system of cone fundamentals does not distinguish between sexes.

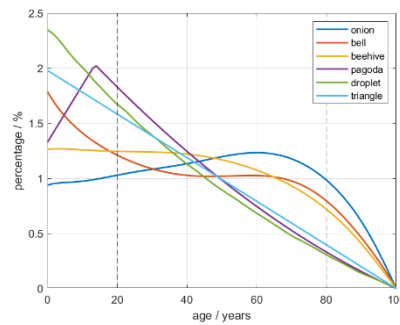


Figure 6 - distribution functions for idealized age class structures often used in demographic studies. In the age range between vertical dashed lines photometric observer functions based on cone fundamentals can be calculated.

Figure 7 shows an example of a population analysis for CIE L41 and the OMI f_V with V_λ as the reference observer. The variation $\Delta_p \approx 12\%$ (Equation 5) is independent of the age class structure and given by the difference between the largest and lowest value in the left graph. Since the reference observer V_λ is close to the 2° cone fundamental observer for an age of 32 years, the weighted population mean $\langle f_V \rangle_{age}$ (Equation 4) is larger for population distributions with higher average age, while the relative variations $\Delta_{age,rel}(f_V)$ (Equation 6) are lower. While $\langle f_V \rangle_{age}$ and $\Delta_{age,rel}(f_V)$ vary with the age class structure of a population, the variations are small compared to the mean values over all age class structures considered.

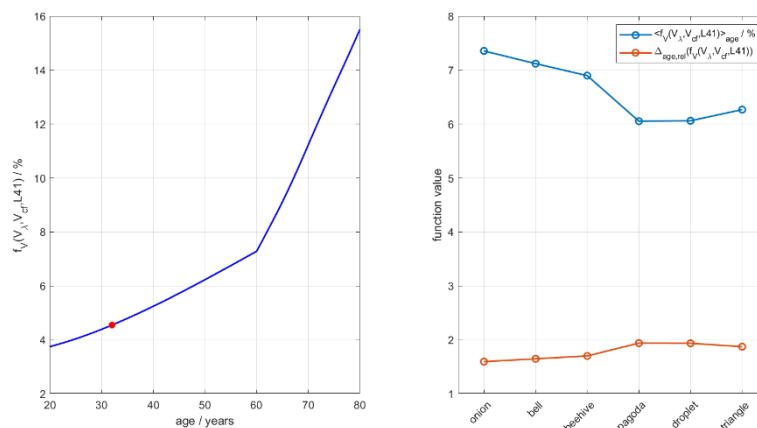


Figure 7 - Example population analysis for spectrum CIE L41 for the OMI f_V with V_λ as reference observer. Left: f_V as a function of cone fundamental observer variation with age. The red dot indicates $V_{cf} = V_F$. Right: Population means (Equation 4) and relative variations (Equation 6) for the age class structures from Figure 6.

5 Characterization of the effect of age dependence of cone fundamental luminous efficiency

In the following we present example statistical analysis for some common “lighting” situations encountered in everyday life. The focus of the paper is to apply the mathematical framework of

sections 3 and 4 to the analysis of the effect of the variation in cone fundamental photometric observer functions with age in different applications. We therefore show here results for two metrics: the OMF $F_V(V_\lambda, V_{cf}, S)$ to indicate the expected variation in brightness perception with respect to the current photometrical system based on V_λ and the OMI $f_V(V_F, V_{cf}, S)$ to analyse the variation in the observer spectral distributions.

The following examples are not meant to be comprehensive for the applications given, but as illustrative examples of the application of the metrics introduced in this paper and the interpretation of the results for distinct sets of spectra.

5.1 Application example: General lighting

Figure 8 shows spectral distributions of lamps often used in “general lighting”, including “daylight”. We excluded here RGB-white LEDs for clarity as those will be featured effectively also in section 5.3. Taking the set of spectral distributions as an example for a possible set representing the application “general lighting”, the statistical analysis from section 4 can be applied to this set of spectra and the variation of cone fundamental photometric observers over the age class structures from Figure 6. Results for $F_V(V_\lambda, V_{cf}, S)$ and $f_V(V_F, V_{cf}, S)$ are presented in Figure 9.

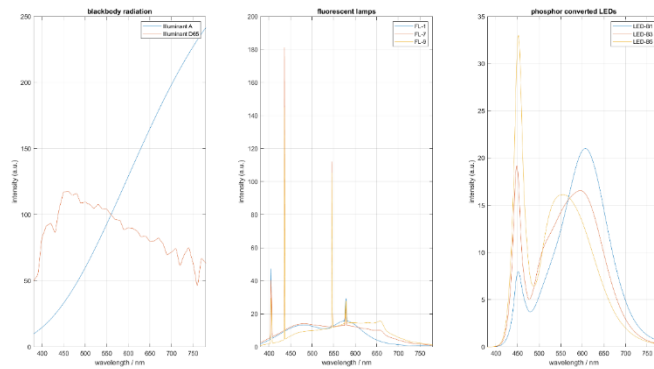


Figure 8 - Example spectral distributions of “white-light” sources encountered in “general-lighting” situations.

For broadband “white light” sources the variation of the metric population means (Equation 4) over the spectra is smaller than the mean mismatch metric value. For both metric examples, the mean values are close to the ones calculated for $S(\lambda) = 1$ (dashed lines) as expected. The variation of $F_V(V_\lambda, V_{cf}, S)$ (Equation 5), measuring the change in perceived brightness compared to V_λ , with age is large over the set of spectra. For $f_V(V_F, V_{cf}, S)$, characterizing the absolute spectral observer differences with respect to V_F other than a pure change in perceived brightness, the variation is small and close to the value for $S(\lambda) = 1$. The metric Δ_p (Equation 5) does not provide interesting information for $F_V(V_{ref}, V_{cf}, S = 1)$ even for broadband spectra, which is expected from the OMF definition (Equation 1) and illustrated by Figure 9.

Table1 gives an overview over the correlations between the various metrics introduced in section 3. As expected, for broadband sources the spectral mismatch indices f_V and f_{V2} are nearly fully correlated while there is a significant anti-correlation with the spectral mismatch factor F_V .

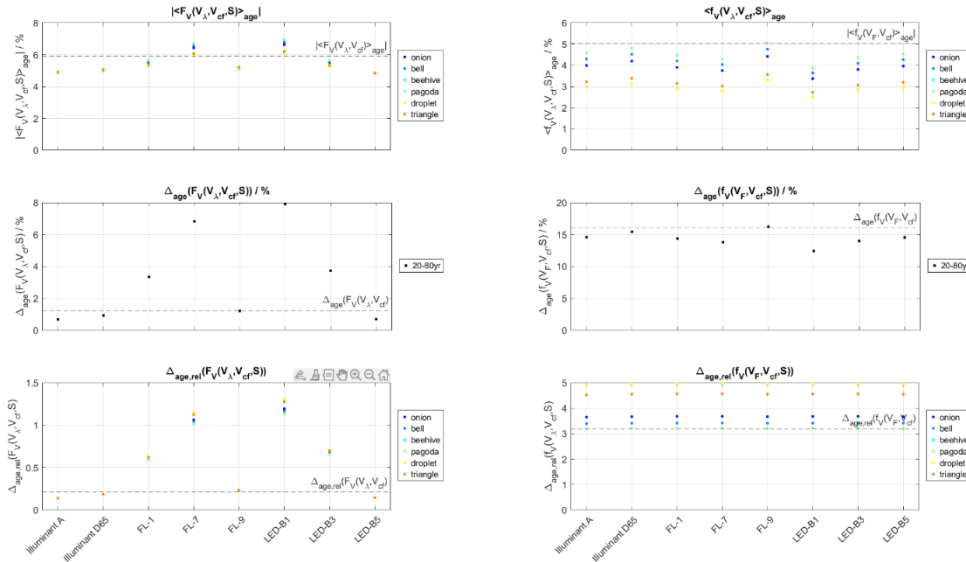


Figure 9 - Statistics from section 4 for $F_V(V_\lambda, V_{cf}, S)$ (left column) and $f_V(V_F, V_{cf}, S)$ (right column) for spectral distributions S from Figure 8 and populations from Figure 6.

Table 1 - Pearson correlation coefficients for the metrics introduced in section 3 for reference observers V_λ and V_F over all spectral distributions from Figure 8 and 2° cone fundamental photometric observers V_{cf} from ages 20 to 80.

Metric	$f_V(V_\lambda, V_{cf})$	$f_{V2}(V_\lambda, V_{cf})$	$F_V(V_\lambda, V_{cf})$	$f_V(V_F, V_{cf})$	$f_{V2}(V_F, V_{cf})$	$F_V(V_F, V_{cf})$
$f_V(V_\lambda, V_{cf})$	1,0	0,8	-0,5	1,0	0,9	-0,5
$f_{V2}(V_\lambda, V_{cf})$	0,8	1,0	-0,5	0,8	0,9	-0,5
$F_V(V_\lambda, V_{cf})$	-0,5	-0,5	1,0	-0,4	-0,4	1,0
$f_V(V_F, V_{cf})$	1,0	0,8	-0,4	1,0	1,0	-0,4
$f_{V2}(V_F, V_{cf})$	0,9	0,9	-0,4	1,0	1,0	-0,4
$F_V(V_F, V_{cf})$	-0,5	-0,5	1,0	-0,4	-0,4	1,0

5.2 Application example: Street lighting

Figure 10 shows spectral distributions of a selection of lamps encountered in street lighting, including three single colour LED-spectra of a typical traffic light, taken from (TAPIA 2015).

Taking this set of spectral distributions as an example for a possible set representing the application “street lighting”, the statistical analysis from section 4 can be applied to this set of spectra and the variation of cone fundamental photometric observers over the age class structures from Figure 6. Results for $F_V(V_\lambda, V_{cf}, S)$ and $f_V(V_F, V_{cf}, S)$ are presented in Figure 11.

Comparing results for the two metrics shows that, for this application, the metrics V_F and f_V “measure” different properties of the observers as large (small) values occur for different lamp spectra. In particular, f_V tends to be smaller for narrow band spectra, while F_V is typically larger (compare section 3.4.), while for “broadband” spectra the behaviour is typically reversed. Metric values characteristic for the application can for example be derived by taking mean values and max values of Δ_{age} (middle row of Figure 11) over all spectra. Other than in section 5.1 above, the metric values for $S(\lambda) = 1$, corresponding to a direct comparison of the observers, provides no useful application for this application. This is expected for any application featuring highly structured and/or narrow-band spectral distributions. The metric $\Delta_{age}(F_V(V_\lambda, V_{cf}, S))$ can be used to identify lamp types for which the variation over observers in brightness perception is minimal. Those lamp types would be candidates for “universal” sources that would minimize the impact of observer difference with age on the application.

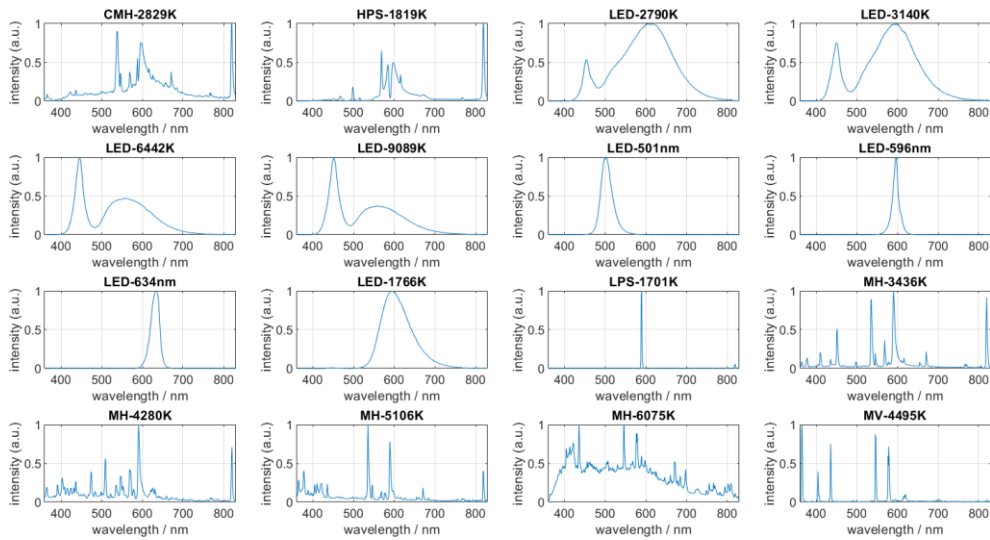


Figure 10 - Example spectra of street lights and traffic lights. CMH: compact metal halide, HPS: high pressure sodium, LED: light emitting diode, LPS: low pressure sodium, MH: metal halide, MV: mercury vapor. Numbers indicate correlated colour temperatures or peak wavelengths as given in the name of the source in the spectral database (TAPIA 2015) and are for rough information purposes only.

For the heterogeneous set of spectra characterizing the “street- and traffic lighting” application, the values of the different metrics for the set of observers and spectra considered are mostly uncorrelated (see Table 2). This illustrates that the different metrics in general measure different aspects of the effect of the spectral observer differences (Figure 1) for given (sets of) spectra. Correlation is strong for different choices of the reference observer. This reflects the fact that, if there are more than two observers, the metrics variation over the set of observers is, up to a systematic offset, largely independent of the choice of the reference observer.

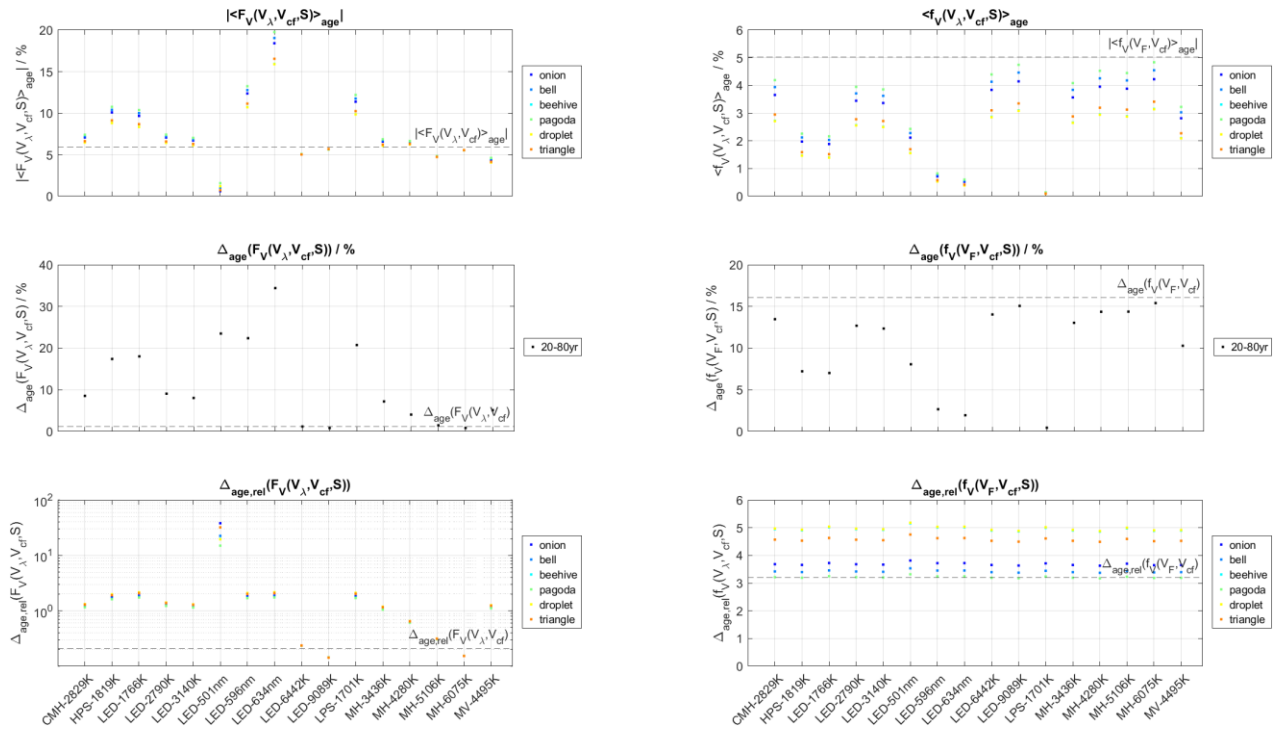


Figure 11 - Statistics from section 4 for $F_V(V_\lambda, V_{cf}, S)$ (left column) and $f_V(V_F, V_{cf}, S)$ (right column) for spectral distributions S from Figure 10 and populations from Figure 6.

Table 2 - Pearson correlation coefficients for the metrics introduced in section 3 for reference observers V_λ and V_F over all spectral distributions from Figure 10 and 2° cone fundamental photometric observers V_{cf} from ages 20 to 80.

Metric	$f_V(V_\lambda, V_{cf})$	$f_{V2}(V_\lambda, V_{cf})$	$F_V(V_\lambda, V_{cf})$	$f_V(V_F, V_{cf})$	$f_{V2}(V_F, V_{cf})$	$F_V(V_F, V_{cf})$
$f_V(V_\lambda, V_{cf})$	1,0	0,1	-0,1	0,9	0,4	0,1
$f_{V2}(V_\lambda, V_{cf})$	0,1	1,0	0,7	0,3	0,8	0,7
$F_V(V_\lambda, V_{cf})$	-0,1	0,7	1,0	0,0	0,4	1,0
$f_V(V_F, V_{cf})$	0,9	0,3	0,0	1,0	0,6	0,0
$f_{V2}(V_F, V_{cf})$	0,4	0,8	0,4	0,6	1,0	0,4
$F_V(V_F, V_{cf})$	0,1	0,7	1,0	0,0	0,4	1,0

5.3 Application Example: Displays (coloured Light)

Figure 12 shows typical spectral distributions for two commonly used display technologies, liquid crystal displays (LCD) and organic light emitting diode displays (OLED). Taking this set of spectral distributions as an example for a possible set representing the application “information display”, the statistical analysis from section 4 can be applied to this set of spectra and the variation of cone fundamental photometric observers over the age class structures from Figure 6. Results for $F_V(V_\lambda, V_{cf}, S)$ and $f_V(V_F, V_{cf}, S)$ are presented in Figure 13.

For LCD and OLED, the results do not depend significantly on the display technology. For “white” display settings, the value of Δ_{age} is minimal for the OMF, while it approaches the pure observer mismatch value for the OMI, which is typical for a broadband spectrum. For the blue primaries, Δ_{age} as well as $\langle X_V \rangle_{age}$ is maximal, reflecting the fact that this spectral distribution is rather narrowband and concentrated in a spectral range where the spectral differences between observers is large (see Figure 1). The blue primaries are an example where values for $f_V(V_F, V_{cf}, S)$ can exceed the spectrum independent values $f_V(V_F, V_{cf}, S = 1)$ for a narrow band source, which is in general a clear indication of a strong spectral variation of observers over the spectral range of the source.

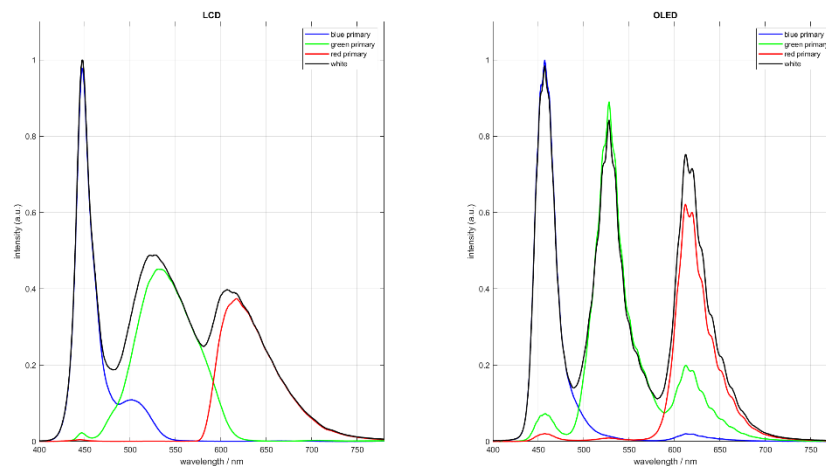


Figure 12 - Example spectral distributions of an LCD display (left) and an OLED display (right).

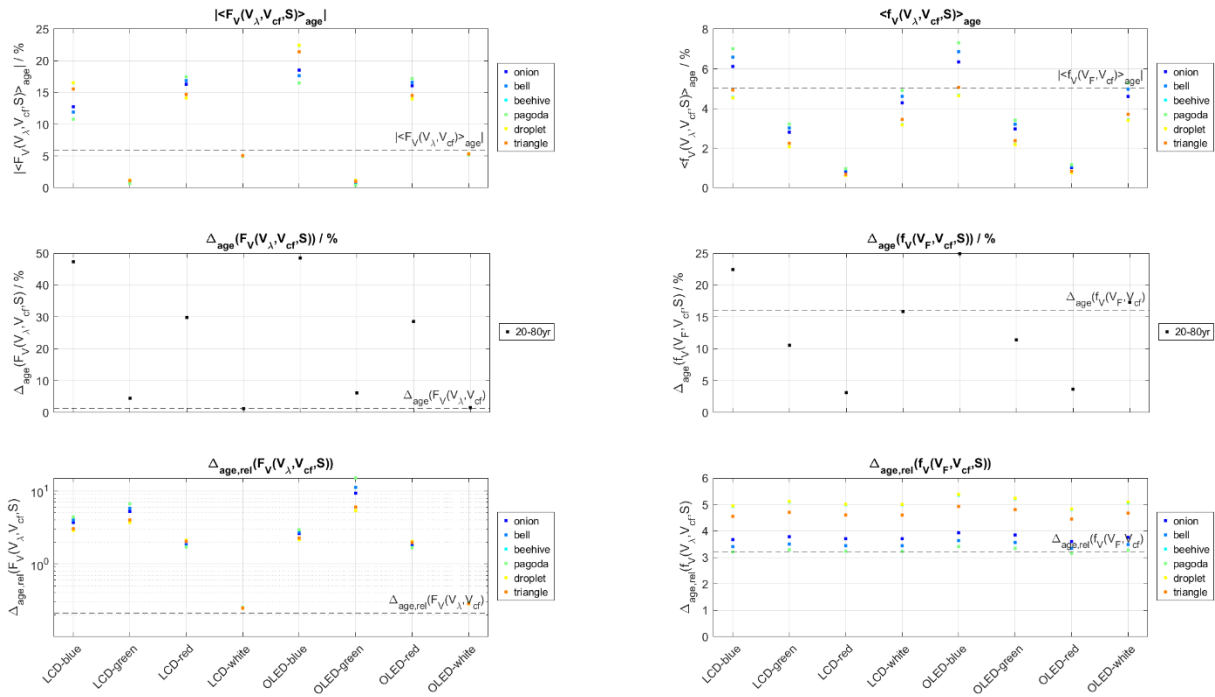


Figure 13 - Statistics from section 4 for $F_V(V_\lambda, V_{cf}, S)$ (left column) and $f_V(V_F, V_{cf}, S)$ (right column) for spectral distributions S from Figure 12 and populations from Figure 6.

Correlations between the various metrics for this particular application are given in Table 3. Again, there is no correlation between the observer mismatch indices, indicating that those “measure” different properties of the observers with respect to the application. The correlation is in general significant id only the reference observer is changed and there is some significant correlation between f_V and F_V for the case of reference observer V_λ that is mostly related to the strong variation between observers in the blue spectral region discussed above.

Table 3 - Pearson correlation coefficients for the metrics introduced in section 3 for reference observers V_λ and V_F over all spectral distributions from Figure 12 and 2° cone fundamental photometric observers V_{cf} from ages 20 to 80.

Metric	$f_V(V_\lambda, V_{cf})$	$f_{V2}(V_\lambda, V_{cf})$	$F_V(V_\lambda, V_{cf})$	$f_V(V_F, V_{cf})$	$f_{V2}(V_F, V_{cf})$	$F_V(V_F, V_{cf})$
$f_V(V_\lambda, V_{cf})$	1,0	0,0	0,3	0,3	0,2	-0,2
$f_{V2}(V_\lambda, V_{cf})$	0,0	1,0	0,5	0,1	0,6	0,6
$F_V(V_\lambda, V_{cf})$	0,3	0,5	1,0	-0,5	-0,2	0,6
$f_V(V_F, V_{cf})$	0,3	0,1	-0,5	1,0	0,8	-0,7
$f_{V2}(V_F, V_{cf})$	0,2	0,6	-0,2	0,8	1,0	-0,1
$F_V(V_F, V_{cf})$	-0,2	0,6	0,6	-0,7	-0,1	1,0

6 Conclusion

In this paper we present a mathematical framework intended to allow a quantitative comparison of action spectra, in particular photometric- or colorimetric observers based on CIE cone fundamentals, and the impact of those spectral differences on a given application defined by a set of characteristic spectral distributions. Three “spectral mismatch” comparison metrics for a pair of action spectra were introduced, the spectral mismatch factor F_V and two spectral mismatch indices f_V and f_{V2} that are sensitive to different aspects of the spectral differences. While is F_V specific for photometric applications, the indices f_V and f_{V2} could also be applied to other types of action spectra.

The problem of comparing distributions of action spectra with respect to particular applications is intrinsically high dimensional including the spectral dimension, the parameters characterising the distribution of action spectra and the size of the set of spectral distributions characterizing an application. In the example of the variation of 2° cone fundamental photometric observers with age we demonstrated how simple statistical evaluations of the proposed spectral mismatch metrics can be used to derive characteristic “benchmark” values for a set of observers and spectral distributions, how the different metrics measure different aspects of the observer spectral differences and how the metrics can help in predicting effects of observer differences on a given applications or can facilitate the choice of light sources that minimize the impact of observer differences for a given application.

References

- CIE 1926. Principales décisions (6^e Session, 1924) CIE Sixième Session, Genève, Juillet, 1924. Recueil des Travaux et Compte Rendu de Séances Huitième Session, Cambridge, Septembre, 19-29, 1931.
- CIE 2006. CIE 170-1:2008. Fundamental Chromaticity Diagram with Physiological Axes – Part 1. Vienna: CIE.
- CIE 2015. CIE 170-2:2015. Fundamental Chromaticity Diagram with Physiological Axes – Part 2: Spectral Luminous Efficiency Functions and Chromaticity Diagrams. Vienna: CIE.
- CIE 2018. CIE 015:2018. Colorimetry, 4th Edition. Vienna: CIE.
- CIE 2023. CIE 251:2023. LED Reference Spectrum for Photometer Calibration. Vienna: CIE.
- FERRERO, A., KOKKA, A., PULLI, T., POIKONEN, T., SCHNEIDER, T., STUKER, F., BLATTNER, P., PONS, A., IKONEN, E., 2019. Definition of spectral mismatch index for spectral power distributions. *CIE x046:2019 Proceedings of the 29th Session of the CIE Washington D.C., USA, June 14 – 22, 2019*, 85-92. DOI 10.25039/x46.2019.OP15
- SHITOMI, H. 2023. Metrological Impact of Introducing Cone Fundamental-Based Photometry as the Basis to Derive Photometric Units. In: *Proceedings of the 30th Session of the CIE, Ljubljana, Slovenia, September 15-23, 2023*. Vienna: CIE, 45–52.
- TAPIA, C. 2015. https://quaix.fis.ucm.es/lamps_spectra